

# Effect of Reacetylation and Degradation on the Chemical and Crystal Structures of Chitosan

Gao Qun, Wan Ajun, Zhang Yong

Department of Chemistry, School of Chemistry and Chemical Technology, Shanghai Jiao Tong University, Shanghai 200240, China

Received 4 December 2005; accepted 2 August 2006

DOI 10.1002/app.25711

Published online in Wiley InterScience (www.interscience.wiley.com).

**ABSTRACT:** The changes of chemical and crystal structures of the reacetylation and degraded chitosans caused by sonication, acid hydrolysis, and H<sub>2</sub>O<sub>2</sub> oxidation were studied systematically. During the reacetylation of chitosan, acetic anhydride can result in the degradation of chitosan when its concentration exceeds a certain value (the acetic anhydride/amine ratio > 0.3). Three crystalline polymorphs appear during the reacetylation process of chitosans that the degree of deacetylation (DD) range from 94 to 5%. The increase of acetyl group leads to a notable crystal structure transition from crystal "Form II" with constrained chain conformation to "Form I" having a more

extended chain structure, and finally to a crystalline form similar to that of chitin. The DD of chitosan is not altered by sonication and acid hydrolysis, but decrease obviously because of deamination occurring in the chain scission of H<sub>2</sub>O<sub>2</sub> oxidation. The crystallinity increases with the decreasing of molecular weight for sonication and acid hydrolysis, whereas a deeper degradation by H<sub>2</sub>O<sub>2</sub> will decrease the crystallinity. © 2007 Wiley Periodicals, Inc. *J Appl Polym Sci* 104: 2720–2728, 2007

**Key words:** chitosan; reacetylation; degradation; degree of deacetylation; molecular weight; crystal structure

## INTRODUCTION

Chitosan, (1 → 4)-2-amido-2-deoxy-β-D-glucan, has been widely used in water treatment, pulp and paper, medicine, cosmetics, agriculture, food, biotechnology, etc. The effectiveness of chitosan and its derivatives has been found to be dependent not only on their molecular weights and degree of deacetylation (DD) but also on the molecular conformation of chitosan together with its packing arrangement.<sup>1–3</sup> Therefore, structure study of chitosan becomes important for better understanding of its functions and utilization.

Many different diffraction experiments have been undertaken in an attempt to elucidate the molecular geometry of chitosans in solid state, which were obtained from diverse degradation methods. These studies have revealed at least six crystal polymorphs for chitosan: "tendon chitosan,"<sup>4</sup> "annealed,"<sup>5</sup> 'I-2', 'L-2',<sup>6</sup> "Form I" and "Form II."<sup>7</sup> The single molecular chain in these polymorphs has been observed to be an extended twofold helical structure similar to chitin and cellulose, but the diversity in cell parameters of

chitosan may reflect the different conformation and packing versatility of this biopolymer. Ogawa et al.<sup>8</sup> proposed that the lattice parameters for a number of chitosan specimens were classified into two, hydrated and anhydrous. Polymers in them have the same extended twofold helical structure, while the packing arrangements and water contents are quite different. Four chitosan conformations have been found in the crystals of chitosan-acid salts, and it depends mainly on the kinds of acid, but in the case of some acid salts, it depends on concentration of acid or temperature at salt preparation.<sup>9</sup> However, the polymorphs of chitosan is far from being fully understood, especially the transformation between the two polymorphs of chitosan.

It is known that the reacetylation process and degradation will contribute to chemical and crystal structure changes. However, up to now, few researches focused on comparison of effects of reacetylation and degradation methods on the chemical and crystal structures of chitosans. In this study, we provide more documents on the changes of chemical structure and crystal polymorph of chitosans that were obtained by three often-used degradation methods (hydrochloric acid hydrolysis, hydrogen peroxide oxidation, and sonication) as well as reacetylation process. The main job of this work was to look for the influence of reacetylation process and degradation methods on the solid state structure, i.e., crystal structure transformation of chitosan.

Correspondence to: W. Ajun (wanajun@sjtu.edu.cn).

Contract grant sponsor: National Natural Science Foundation of China; contract grant number: 20376045.

Contract grant sponsor: Science and Technology Committee, Shanghai; contract grant number: 0452nm037.

## EXPERIMENTAL

### Preparation of various DD chitosans

The chitosan samples of various DDs but same molecular weights were prepared by homogeneous reacetylation.<sup>10</sup> A commercial sample of chitosan low molecular weight chitosan (LMCS) (DD94%) was dissolved in 0.1M CH<sub>3</sub>COOH. The solution was passed through a filter paper to remove insoluble material and gel particles, then precipitated by addition of NaOH solution (1M), washed with deionized water until neutral, and dried at 60°C under vacuum.

Aliquots (2 g) of the products were redissolved in 0.1M CH<sub>3</sub>COOH (200 mL) and diluted with methanol (350 mL). Then to each solution was added, with vigorous stirring, a further 50 mL of methanol containing the calculated amount of acetic anhydride required to meet the target level of *N*-acetylation. After standing at room temperature for 24 h, the *N*-acetylated products were precipitated by the addition of concentrated NH<sub>4</sub>OH solution, filtered off, washed to neutral with 75% aqueous methanol, and then dried at 60°C under vacuum.

### Ultrasonic degradation

Two commercial chitosan samples (Jinhu, China) were prepared from crab shell, with the molecular weights of 1880 KDa (HMCS; high molecular weight chitosan) and 1240 KDa (LMCS) and the DD of 90 and 94%, respectively. One percentage of original chitosan was dissolved in acetic acid aqueous solution (5%, v/v), and then ultrasonically degraded at 250 W with a frequency of 40 KHz (CQX25-06, Branson Ultrasonics (Shanghai), China) for various time (0–20 h) at 60°C. After the degradation, the chitosans were precipitated with 1M NaOH solution and washed with water until neutral, and then dried at 60°C under vacuum.

Polydispersity of untreated and untrasonic degraded chitosans were determined by gel permeation chromatography (series 200, PerkinElmer, MA). The eluent was 0.2M CH<sub>3</sub>COOH/0.1M CH<sub>3</sub>COONa aqueous solution, sample concentration of 0.1% (w/v) was loaded, and eluted with a flow rate of 0.5 mL/min at 40°C. Two serial columns packed with PL gel and 10 μm mixed-B columns were used; the elution peak was detected by a PerkinElmer series 200 Refractive index Detector.

### Hydrolysis of chitosan with HCl

HCl hydrolytic fragmentation was carried out in a 250-mL spherical flask equipped with a vertical condenser. An aliquot of 5 g purified chitosan powder was suspended in 100 mL 2.5M HCl solution with constant stirring at 60°C for different durations. The

reaction time was variable, assigned as 1, 2, 4, 6, 10, and 14 h, to obtain the materials with different degrees of polymerization. At the end of predetermined time, the reaction mixture was neutralized with 5M NaOH to pH = 8–9, added 400 mL methanol, filtered off, washed with 75% aqueous methanol, and then dried at 60°C under vacuum.

Chitosan/HCl salt was prepared by dissolving the degraded chitosan (degradation time 2 h) in 0.1M HCl solution, filtered off and the solution was dried at 60°C under vacuum.

### Degradation of chitosan by hydrogen peroxide

The reaction conditions were identical to the HCl degradation described earlier. During the reaction, hydrogen peroxide (30% H<sub>2</sub>O<sub>2</sub>) was added slowly into the solution to obtain a final concentration of 2.5%. After the reaction, the solution was neutralized with 5M NaOH, added 400 mL methanol, filtered off, washed with 75% aqueous methanol, and then dried at 60°C under vacuum.

### DD determination

The potentiometry was used to determine the DD of these chitosans.<sup>11</sup> An aliquot of 0.5-g dry chitosan was accurately weighted and dissolved in 0.1M HCl. The solution was titrated with 0.1M NaOH. The DD was calculated as follows:

$$\text{NH}_2\% = \frac{(C_1V_2 - C_2V_1)0.016}{G(100 - W)} \times 100 \quad (1)$$

where  $C_1$  is the concentration of HCl (mol L<sup>-1</sup>);  $C_2$ , the concentration of NaOH (mol L<sup>-1</sup>);  $V_1$ , the volume of HCl (mL);  $V_2$ , the volume of NaOH;  $G$ , the sample weight (g);  $W$ , the water percentage of sample (%); and 0.16 is the weight of NH<sub>2</sub> equal to 1 mL 0.1M HCl (g). Then

$$\text{Degree of deacetylation}(\%) = \text{NH}_2\%/9.94\% \times 100\% \quad (2)$$

where 9.94% is the theoretical NH<sub>2</sub> percentage of chitosan.

### Molecular weight determination

The molecular weight of chitosan was determined by the capillary viscometry method using an Ubbelohde viscometer at 25°C. Five concentrations were prepared by the dilution of the degraded chitosan solution with a 0.1M CH<sub>3</sub>COOH–0.2M NaCl solution. The specific viscosity ( $\eta_{sp}$ ) at different concentrations was then measured and the intrinsic viscosity ( $\eta$ ) was obtained by extrapolating the linear plot of  $\eta_{sp}/c$  vs.  $c$

to the zero concentration. The viscosity average molecular weight ( $\bar{M}_v$ ) was then calculated using the Mark-Houwink equation  $[\eta] = kM^a$ , in which the constants  $k$  and  $a$  depended on the DD as follows<sup>12</sup>:

$$K = 1.64 \times 10^{30} \times DD^{14} \quad (3)$$

$$a = -1.02 \times 10^{-2} \times DD + 1.82 \quad (4)$$

#### Fourier transform infrared spectroscopy

Fourier transform infrared (FTIR) spectra of the samples were obtained with a PerkinElmer spectrometer 1600 $\times$  with a resolution of 4  $\text{cm}^{-1}$  and 32 accumulations. KBr pellets were prepared in the usual way of about 1 mg of the sample mixing with 100 mg of KBr. Spectral scanning was done in the range between 4000 and 500  $\text{cm}^{-1}$ .

#### Powder X-ray diffraction

The X-ray diffraction (XRD) measurements of chitosans were performed on a X-ray Diffractometer (Model 6000, Shimadzu, Japan) with scanning scope of  $3^\circ < 2\theta < 40^\circ$  scanning rate of  $6^\circ/\text{min}$ , using Cu K $\alpha$  radiation.

## RESULTS AND DISCUSSION

#### Effect of reacetylation process on the molecular weight and DD of chitosans

The preparation of various DD chitosans was performed by a homogeneous reaction, which the amine group reacting with the calculated amount of acetic anhydride. The molar ratio of acetic anhydride/amine group ranges from 0.1 to 2.0. As the molar ratio is higher than 0.7, the acetylated chitosans were insoluble in HCl solution and any other aqueous solution,

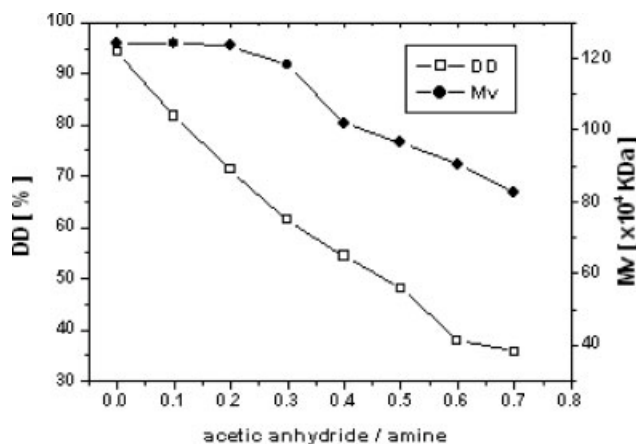


**Figure 1** Effect of reacetylation on degree of deacetylation and molecular weight of chitosans.

and then the DD and the average viscosity molecular weight cannot be determined by potentiometry and capillary viscometry methods as mentioned earlier. Figure 1 shows the change of DD varying with molar ratio of acetic anhydride/amine.

Generally, the *N*-acetylation of chitosan is the main method to prepare chitosans with different DD but same molecular weights. But in our study (Fig. 1), with the increase of the molar ratio of acetic anhydride/amine, the molecular weight of chitosan first remains constant (0.1–0.3) and then linearly decreases. It indicates that acetic anhydride can result in a degradation of chitosan when its concentration exceeds a certain value ( $>0.3$ ).

As can be seen from Figure 1 and Table I, the decrease of DD with the increase of molar ratio of acetic anhydride/amine is nonlinear.  $\Delta DD$ , which denotes the degree of substitution of *N*-reacetylation caused by 0.1M acetic anhydride decreases gradually (Table I). It indicates that the steric hindrance of acetyl groups is against the reaction of acetic anhydride

**TABLE I**  
The Degrees of Deacetylation and Molecular Weights After Reacetylation Reaction

	Acetic anhydride/amine	Degree of deacetylation	$\Delta DD^a$	Molecular weight ( $\times 10^4$ ; KDa)	Solubility in 0.1M HCl
D94	0	94		124	s
D82	0.1	82	12	124	s
D71	0.2	71	11	124	s
D61	0.3	61	10	118	s
D54	0.4	54	7	102	s
D48	0.5	48	6	96	s
D38	0.6	38	10	90	s
D36	0.7	36	2	83	s
D25	0.8	25			Swelling
D5	1.5	5			n
D4	2.0	4			n

s, soluble; n, insoluble in 0.1M HCl solution.

<sup>a</sup> The decrease of DD when the molar ratio of acetic anhydride/amine increase 0.1.

and amine group of chitosan. The nucleophilic ability of the amine group and the spatial screening of the molecular conformation on the amine group have a profound influence on the degree of substitution of *N*-acetylation. The increase of the acetic anhydride concentration in the solution corresponds to the increase of acetic acid concentration. More protonated amine groups will decrease the nucleophilic ability of the amine group, and counter-ions will screen the protonated amine group and make the molecules conformation changing from extended to contracted.<sup>13</sup> All these result in the decrease of degree of substitution of *N*-reacetylation ( $\Delta$ DD).

### Effect of reacetylation process on the crystal structure of chitosan

The crystal structure of chitosan has been studied by many researchers as mentioned earlier, but little work has focused on the effect of reacetylation on the crystal structure of chitosan. In our study, we prepared a series of chitosans with a broad range of DD (from 5 to 94%) and studied their crystal structure changes by XRD measurement. As shown in Figure 2, there are three distinct polymorphs in the reacetylation process. Compare the cell parameters of the six polymorphs that have been proposed for chitosan: "tendon chitosan," "annealed," 'I-2', 'L-2', "Form I" and "Form II" with our data, it is consistent with the "Form I" and "Form II" polymorphs reported by Samuels.<sup>7</sup> The "Form I" crystal is orthorhombic having unit cell of  $a = 7.76 \text{ \AA}$ ,  $b = 10.91 \text{ \AA}$ , and  $c = 10.30 \text{ \AA}$ . The strongest reflection falls at  $2\theta = 11.4^\circ$  ( $d = 7.76 \text{ \AA}$ ), which is assigned to (100) reflection. The "Form II" crystal is also orthorhombic having a unit cell of  $a$

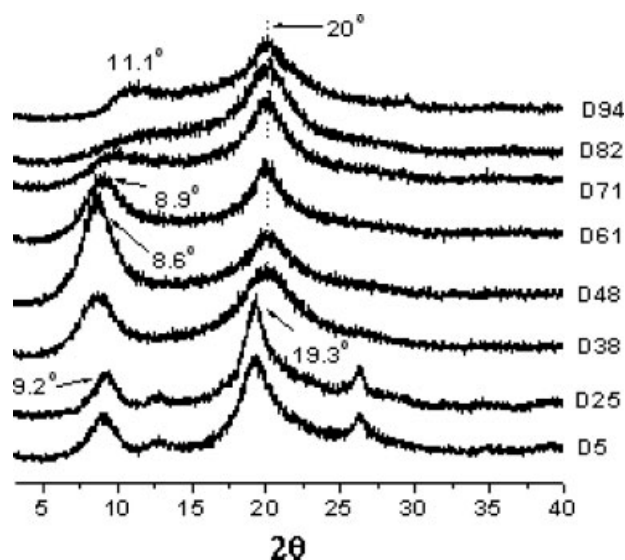


**Figure 2** X-ray diffraction patterns of chitosans prepared by reacetylation reaction.

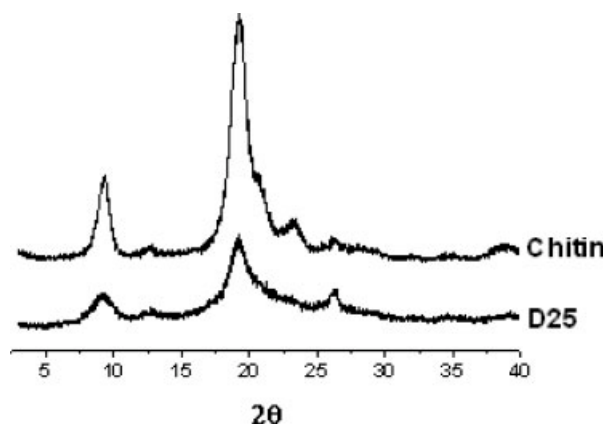


**Figure 3** X-ray diffraction patterns of chitin and chitosan D25.

$= 4.40 \text{ \AA}$ ,  $b = 10.0 \text{ \AA}$ , and  $c = 10.30 \text{ \AA}$  (fiber axis). The strongest reflection appears at  $2\theta = 20.1^\circ$  ( $d = 4.42 \text{ \AA}$ ), which also corresponds to the (100) reflection. As can be seen from Figure 2, the original chitosan (D94) shows the strongest reflection at  $2\theta = 20^\circ$ , coinciding with the pattern of the "Form II" crystal. With the decrease of DD, the intensity of reflection at around  $2\theta = 11.1^\circ$ – $8.6^\circ$  first increases remarkably and then decreases slightly. There is an inverse change for the reflection at about  $2\theta = 20^\circ$ . For chitosan D48, the strongest reflection appears at  $2\theta = 8.6^\circ$ , indicating that a crystal structure transition occurs and form a new type of ordering structure like "Form I" although its  $d$ -spacing ( $d = 10.28 \text{ \AA}$ ) is bigger than "Form I" ( $d = 7.76 \text{ \AA}$ ). The "Form II" crystal with constrained chain conformation converted to "Form I," which has a more extended chain structure. As the DD is lower than 25%, the "Form I" crystal converts to a crystal form similar with chitin (Fig. 3), and its crystallinity is clearly increased and it is insoluble in any aqueous acid solution. The only difference is that the crystallinity of chitin is a lot higher than that of acetylated chitosan D25.

It is also observed from Figures 2 and 4 that with the decrease of DD, the crystalline peak of chitosan at  $2\theta = 11.1^\circ$  first gradually shift to  $8.6^\circ$  and then increases to  $9.2^\circ$ , which is because of the larger  $d$ -spacing as a result of the increase in the unit cell dimension with increasing the content of bulky acetyl groups. As DD decreases from 38 to 5%, the more acetyl groups will increase the ordering structure of chitosan molecular chains, which results in the decrease of  $d$ -spacing and forms a more stereoregularity structure.

### Ultrasonic degradation

Ultrasound has great potential for application in polymerization and degradation of polymers. Kasaai<sup>14</sup>

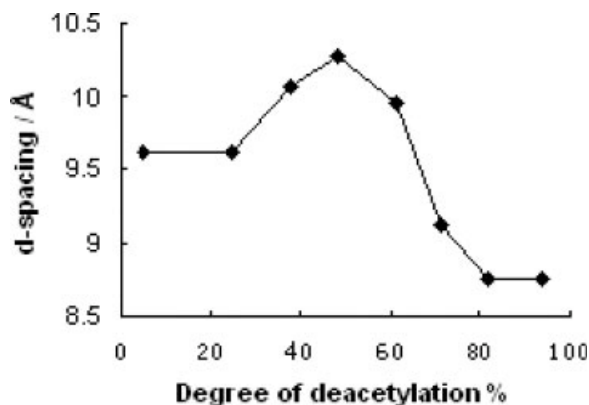


**Figure 4** The relationship between *d*-spacing of the reacylated chitosans calculated from the peaks at low Bragg angles and degree of deacetylations.

demonstrated that ultrasonic power, solution concentration, and solution temperature have great influences on the degradation of chitosans. In this study, two kinds of original chitosans with different molecular weights (HMCS and LMCS) were degraded by sonication and the changes of molecular weight and DD are shown in Figure 5.

The experimental results showed that the DD of chitosans were not altered by sonication. It has been suggested that the sonication is a physical fragmentation. When the chitosan solution is exposed to ultrasound, microbubbles containing dissolved gas or vapor of the liquid are created and these bubbles grow and implode or collapse in microseconds. A strong shear deformation during collapse of the bubbles in the vicinity of cavitations seems to be responsible for the depolymerization of chitosan in aqueous solutions.<sup>15</sup>

It can be seen from Figure 5, the molecular weight of chitosan HMCS decreases linearly with increasing the degradation time, and the molecular weight of chitosan LMCS decreases exponentially with increasing sonication time. The presence of a limiting final molecular weight is typical for the degradation of chitosan.<sup>14–16</sup> For the LMCS, the final molecular weight is 760 KDa after 20 h. However, for the HMCS, it does not exist a final molecular weight and the degradation rate remains constant during the sonication.

The ratio of ultrasonicated to initial molecular weight  $X = M_t/M_0$  of HMCS decreases from  $X = 1$  at  $t = 0$  to  $X = 0.46$  at  $t = 19$  h, whereas for LMCS  $X$  decreases from 1 to 0.61 at  $t = 20$  h. It suggests that the degradation rate of HMCS is faster than that of LMCS under the same conditions.

To elucidate the different degradation plots of the two chitosans, the polydispersity of degraded chitosans was determined by GPC, and the results were shown in Table II. It can be seen that the polydispersity decreases for the ultrasonic degradation chito-

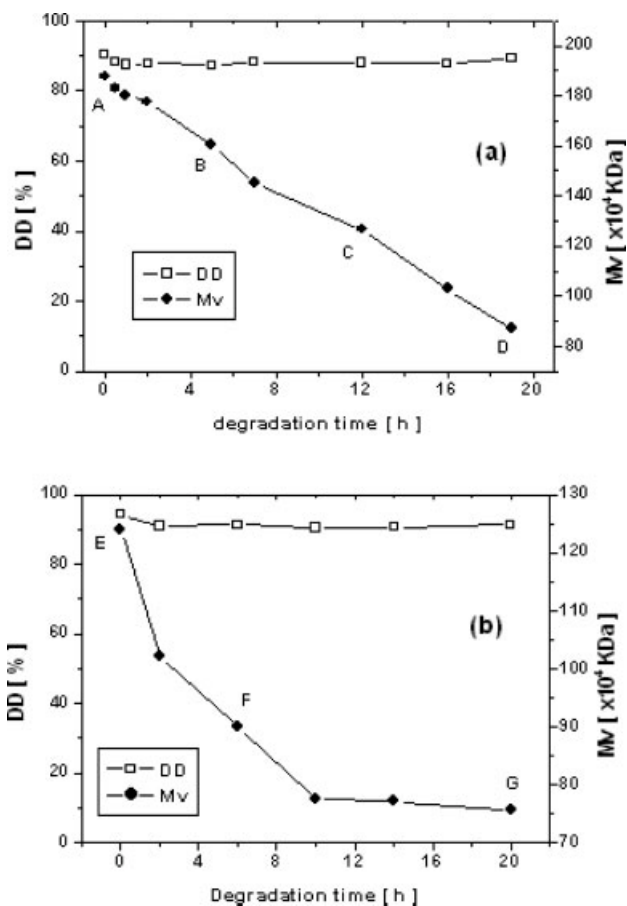


**Figure 5** The molecular weight and degree of deacetylation of chitosans degraded by ultrasonication for original chitosan: (a) HMCS and (b) LMCS.

sans. Original chitosan LMCS (E) has a broader molecular weight distribution than that of Fragment C.

It is known that the larger macromolecules are preferentially fragmented and the presence of a final molecular weight has been attributed to the fact that the sensitive of linear stiff rod macromolecules to ultrasonically generated shear and normal stresses decreases with decreasing molecular weight.<sup>15</sup> The molecular weight of chitosan decreases exponentially with increasing the degradation time for LMCS also indicated that the chain scission are not taken place in

**TABLE II**  
The Polydispersity of Chitosans Degraded by Ultrasonication

Chitosan sample	Polydispersity
A (original chitosan)	4.67
B	4.68
C	4.41
D	4.12
E (original chitosan)	5.43
F	4.93
G	4.90

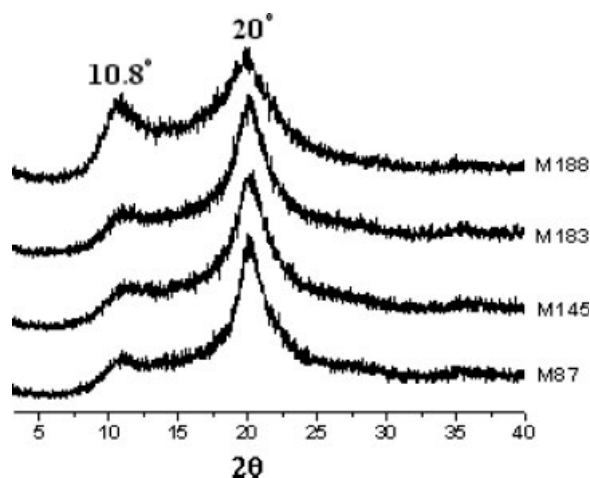


**Figure 6** X-ray diffraction patterns of chitosans degraded by ultrasonication.

the middle of the molecular chain, and the splitting may be much more random and produce more than two fragments from one original molecule.

For the degradation of HMCS, the molecular weight of degraded chitosans did not drop sharply at the beginning of the reaction is attributed to two reasons: (1) the high viscosity of the solution retards the cavitation bubbles grow and collapse, which leads to a decrease in the degradation rate. (2) The stress distribution within the system is not homogeneous because of the strong attenuation of ultrasound waves in the high viscosity solution.<sup>15</sup> With the increase of degradation time, the polydispersity of the degraded chitosan become narrower, the chain scission usually takes place in the middle of molecular chain, the midchain splitting model leading to first-order kinetics appears to be suitable to describe our experimental results.

Samuels<sup>7</sup> reported that the molecular weight of chitosan affected the crystal size and morphological character of its cast film. Several researchers<sup>7,17,18</sup> further observed that crystallinity of membrane increased with decreasing chitosan molecular weight. The XRD measurements of chitosans degraded by ultrasonication are shown in Figure 6. With the decrease of molecular weight, the intensity of reflection at  $2\theta = 10.8^\circ$  decreased, while the strongest reflection at  $2\theta = 20^\circ$  became sharper. It indicates that with the decrease of molecular weight, the larger *d*-spacing unit cells were destroyed and the regularity of the low *d*-spacing structure increased and chitosan molecules preferred to develop a more compact crystalline form.

### HCl degradation

Depolymerization with acid hydrolysis increased with acid concentration and temperature.<sup>19</sup> Chitosan

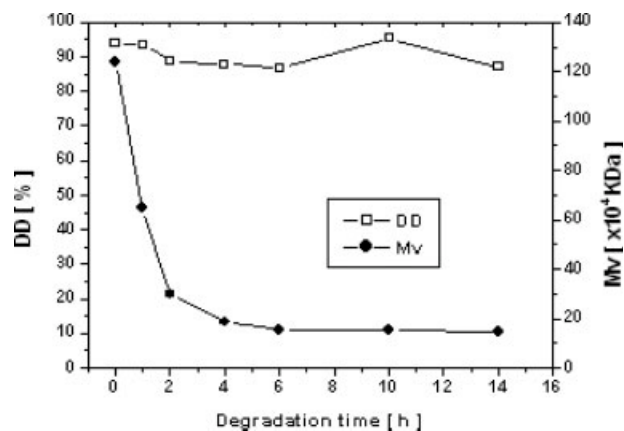
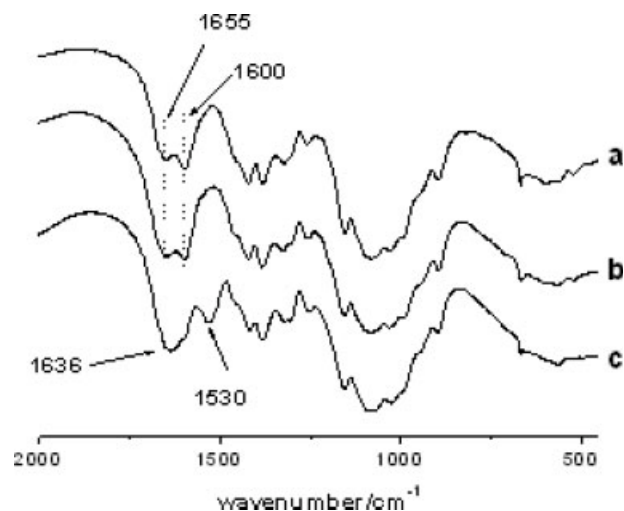


**Figure 7** The molecular weight and degree of deacetylation of chitosans degraded by HCl.

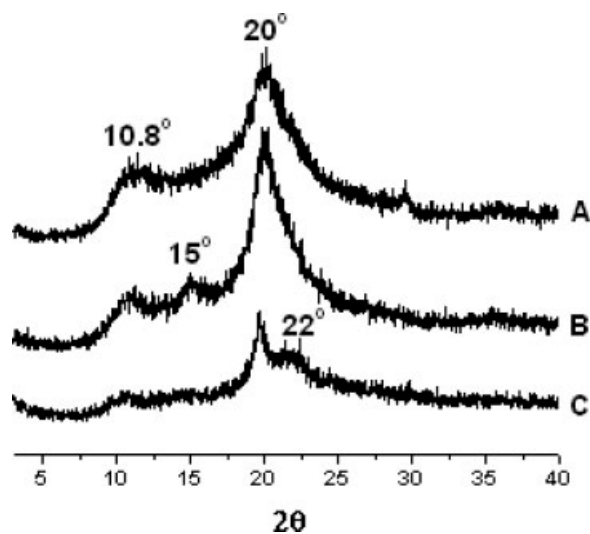
degradation was of first order with HCl.<sup>14</sup> Depolymerization involves two steps: first formation of an intermediate (attachment of a proton ( $H_3O^+$ ) to the glucoside linkage), and second, the splitting of large macromolecular chains into two small ones.

Figure 7 shows that the molecular weight of degraded chitosans dropped sharply at the beginning of the reaction and then reached a plateau after 4 h, i.e., the molecular weight decreased exponentially with degradation time. The final molecular weight of degraded chitosan is 150 KDa under this reaction conditions (2.5M HCl, 60°C). There are no apparent changes of DD during the fragmentation.

The chemical structure of the degraded chitosan and chitosan/HCl salt were analyzed by FTIR (Fig. 8). The FTIR spectra of the degraded chitosans were similar to the original chitosan. The peaks at 1655 and 1600  $cm^{-1}$  are assigned to the carbonyl stretching



**Figure 8** FTIR spectra of chitosans degraded by HCl. (a) original chitosan, (b) degraded chitosans, and (c) degraded chitosans/HCl salt.



**Figure 9** X-ray diffraction patterns of chitosans degraded by HCl. (A) original chitosan, (B) degraded chitosans, and (C) degraded chitosans/HCl salt.

(amide I) and N—H bending of  $\text{NH}_2$ . In contrast, for chitosan/HCl salt, these two bands shifted to  $1636$  and  $1530\text{ cm}^{-1}$ , suggesting the presence of  $-\text{NH}_3^+$ . These two kinds of chitosans dried under acid or neutral conditions formed different crystal structures as shown in Figure 9.

Two crystalline forms of chitosan, hydrated and anhydrous, have been reported by Ogawa et al.<sup>9</sup> The incorporation of bound water molecules into the crystal lattice gives rise to more abundant polymorph. For the degraded chitosan [Fig. 9(B)], it exhibits characteristic peaks at  $2\theta = 10.8^\circ$  and  $20^\circ$ , which coincides with the pattern of 'L-2'-type polymorph. A small peak appears at round  $15^\circ$  ( $d = 5.86\text{ \AA}$ ), that is, the (120) reflection, because of an anhydrous crystal lattice. The anhydrous crystalline form is shown to exhibit minimal chemical and biological activities.<sup>20</sup> Therefore, the degraded chitosan is a mixture of the 'L-2' hydrate and "anhydrous" (annealed) polymorph. For chitosan/HCl salt [Fig. 9(C)], the pattern has four main peaks. When compared with the original chitosan, the peak at  $2\theta = 22^\circ$  rise and the peaks at  $2\theta = 10.8^\circ$  and  $15^\circ$  decrease obviously. It can be considered as a mixture of the "tendon" hydrate and "anhydrous" polymorph. In comparison, chitosan B has a higher crystallinity than chitosan C. During the heterogeneous degradation with HCl, the degradation first took place preferentially in the amorphous region and then proceeded moderately from the edge to the inside of the crystalline.<sup>21</sup> For low molecular weight chitosan, the regularity of the structure increased and chitosan molecules preferred to form a more compact crystalline form. Whereas for chitosan C, the intermolecular N(2)—O(6) hydrogen bonds, which contribute to the three-dimensional stabilizing of crystal struc-

ture of chitosan<sup>9</sup> lose and it makes the molecules cannot form an ordered crystal structure, and result in a low crystallinity.

### $\text{H}_2\text{O}_2$ degradation

$\text{H}_2\text{O}_2$  degradation was performed to obtain chitosans with a much lower molecular weight and the results were shown in Figure 10. It can be seen that the molecular weight of degraded chitosans reached its plateau in the first hour and then remained approximately constant at about  $34\text{ kDa}$ , which is the lowest molecular weight it can be achieved under the reaction condition. The degradation rate was much faster than that of HCl degradation. The participation of  $\text{H}_2\text{O}_2$  in the reaction might be acted as oxidation reagent and catalyst.<sup>14</sup> Generally, hydrogen peroxide produces hydroxyl-free radicals through different ways. The presence of minute amounts of metal salts will catalyze the decomposition of  $\text{H}_2\text{O}_2$  to form hydroxyl-free radicals<sup>22</sup>; hydrogen peroxide ionizes to produce the perhydroxyl anion, which reacts with  $\text{H}_2\text{O}_2$  to form the highly reactive hydroxyl radical ( $\text{HO}\cdot$ ).<sup>21</sup>  $\text{HO}\cdot$  radical is a much more powerful oxidant, and it can abstract hydrogen atoms from the glucosamine residues of chitosan. Then, chitosan molecules will rearrange their structures and break down to form smaller molecules.

Figure 10 also exhibits that, with the increase of degradation time, the DD decreases from 94 to 50%. The FTIR spectra of the degraded chitosans (Fig. 11) show that the intensities of peaks at  $1420\text{ cm}^{-1}$  (symmetrical deformation of  $-\text{CH}_3$  and  $-\text{CH}_2$ ),  $1654\text{ cm}^{-1}$  (amide I), and  $1600\text{ cm}^{-1}$  (N—H deformation of  $-\text{NH}_2$ ) decrease, indicating that the  $\text{COCH}_3$  and  $\text{NH}_2$  groups decrease after the  $\text{H}_2\text{O}_2$  degradation. The deamination suggests that the scission of glycosidic bond is predominantly from H-abstraction at C-1 and

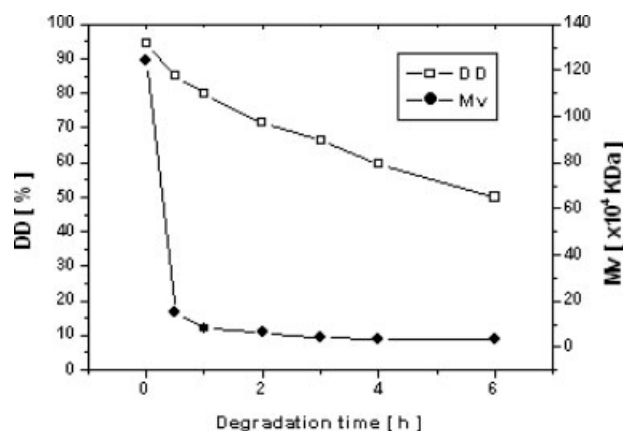


**Figure 10** The degree of deacetylation and molecular weight of chitosans degraded by  $\text{H}_2\text{O}_2$ .

C-2.<sup>21</sup> However, there is no carboxyl band present in the spectra, which is usually formed in the oxidative scission, suggesting that there is no carboxyl group formation under the reaction condition.

Figure 12 shows the XRD patterns of chitosans degraded by H<sub>2</sub>O<sub>2</sub>. The peak intensities of degraded chitosans are significantly lower than those of original chitosan at  $2\theta = 10.8^\circ$  and  $2\theta = 20^\circ$ , and the peak at  $2\theta = 20^\circ$  becomes broad. At the first stage of the degradation (D1), a weak peak appears at  $15^\circ$ , which is an anhydrous crystalline form. This diffraction pattern is similar to the chitosans degraded by HCl except for the decrease in crystallinity. When compared with the increase of crystallinity of chitosans degraded by ultrasonication and HCl hydrolysis, it is indicated that with deeper degradation by H<sub>2</sub>O<sub>2</sub>, the crystal structure was destroyed and finally form an amorphous structure. It implies that it is not a simple relationship between the molecular weight and crystallinity because of the complicated influence factors on the crystal structure, such as chemical structure, DD, degradation method, and degradation condition.

### CONCLUSIONS

The molecular weight, DD, and crystal structure are the important physiochemical properties that greatly influenced the applications of chitosan in many areas. In general, ultrasonication is advantageous over chemical methods because it does not need chemical reagents and will not alter chemical structure, but the preparation of large amounts of chitosans with low molecular weights is less feasible. The degradation rate of oxidative methods is much faster than that of acid hydrolysis, but it is difficult to con-

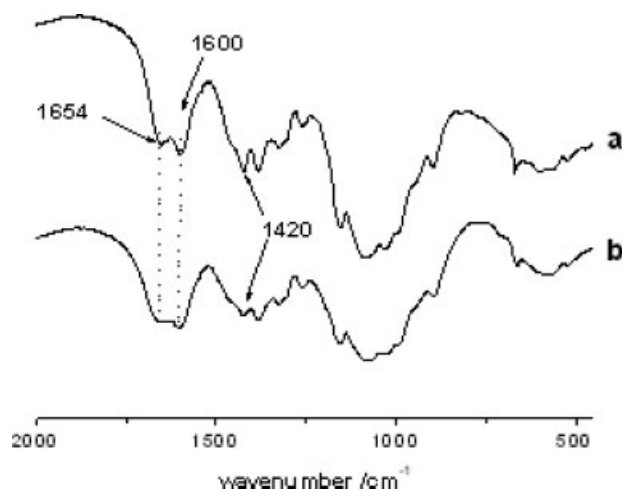


**Figure 11** FTIR spectra of chitosans degraded by H<sub>2</sub>O<sub>2</sub>. (a) original chitosan and (b) degraded chitosans.

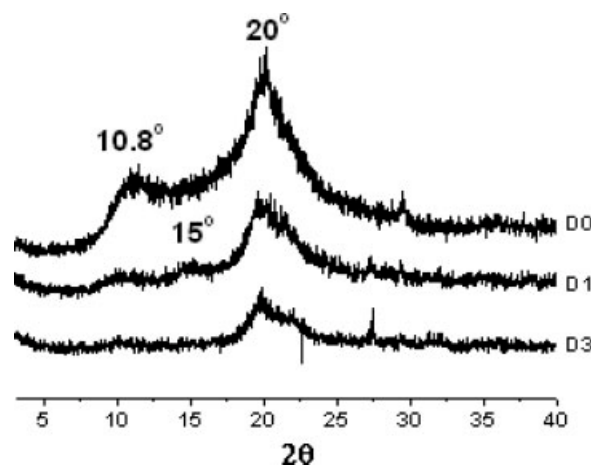


**Figure 12** X-ray diffraction patterns of chitosans degraded by H<sub>2</sub>O<sub>2</sub>. (D0) original chitosan, (D1) chitosan with degradation time of 1 h, and (D3) chitosan with degradation time of 3 h.

trol the reaction process to obtain the desirable molecular weight. The DD of chitosan degraded by H<sub>2</sub>O<sub>2</sub> decreases because the deamination occurs in the chain scission. The XRD determination demonstrates that the changes of molecular weight and DD have a notable influence on the crystal structure of chitosan. With the decrease of DD, the reacetylation of chitosan resulted in a polymorph transition from constrained chain conformation "Form II" to a more extended chain structure "Form I," and further to develop a crystal structure similar to that of chitin. The crystallinity will increase with the decreasing molecular weight for sonication and acid hydrolysis, whereas a deeper degradation by H<sub>2</sub>O<sub>2</sub> will decrease the crystallinity. Therefore, the changes of physiochemical properties resulted from the reacetylation and different degradation methods should be well considered during the application of chitosans.

### References

- No, H. K.; Park, N. Y.; Lee, S. H.; Meyers, S. P. *Int J Food Microbiol* 2002, 74, 65.
- Tomihata, K.; Ikada, Y. *Biomaterials* 1997, 18, 567.
- Majeti, N. V.; Kumar, R. *React Funct Polym* 2000, 46, 1.
- Clark, G.; Smith, A. F. *J Phys Chem* 1937, 40, 863.
- Ogawa, K.; Hirano, S.; Miyanishi, T.; Yui, T.; Watanabe, T. *Macromolecules* 1984, 17, 973.
- Sakurai, K.; Shibano, T.; Kimura, K.; Takahashi, T. *Sen-I Gakkaishi* 1985, 41, T-361.
- Samuels, R. J. *J Polym Sci Polym Phys* 1981, 19, 1081.
- Okuyama, K.; Noguchi, K.; Kanenari, M.; Egawa, T.; Osawa, K.; Ogawa, K. *Carbohydr Polym* 2000, 41, 237.
- Ogawa, K.; Yui, T.; Okuyama, K. *Int J Biol Macromol* 2004, 34, 1.
- Berth, G.; Dautzenberg, H. *Carbohydr Polym* 2002, 47, 39.
- Lin, R.; Jiang, S.; Zhang, M. *Chem Bull* 1992, 3, 39.



12. Wang, W.; Bo, S. Q.; Li, S. Q.; Qin, W. *Int J Biol Macromol* 1991, 13, 281.
13. Tsaih, M. L.; Chen, R. H. *Int J Biol Macromol* 1997, 20, 233.
14. Kasai, M. R. Ph.D. Dissertation, University Laval, Canada, 1999, AAINQ51261.
15. Baxter, S.; Zivanovic, S.; Weiss, J. *Food Hydrocolloid* 2005, 19, 821.
16. Chen, R. H.; Chang, J. R.; Shyur, J. S. *Carbohydr Res* 1997, 299, 287.
17. Ogawa, K.; Yui, T.; Miya, M. *Biosci Biotech Biochem* 1992, 56, 858.
18. Hwang, K. T.; Kim, J. T.; Jung, S. T.; Cho, G. S.; Park, H. J. *J Appl Polym Sci* 2003, 89, 3476.
19. Kikkawa, Y.; Kawada, T.; Furukawa, I.; Sakuno, T. *J Fac Agric* 1990, 26, 9.
20. Yui, T.; Imada, K.; Okuyama, K.; Obata, Y.; Suzuki, K.; Ogawa, K. *Macromolecules* 1994, 27, 7601.
21. Qin, C. Q.; Dua, Y. M.; Xiao, L. *Polym Degrad Stab* 2002, 76, 211.
22. Chang, K. L.; Tai, M. C.; Cheng, F. H. *J Agric Food Chem* 2001, 49, 4845.